World Academy of Science, Engineering and Technology
International Journal of Mechanical and Mechatronics Engineering
Vol:5, No:12, 2011

Seismic Response Reduction of Structures using Smart Base Isolation System

H.S. Kim

***Abstract*—**In this study, control performance of a smart base isolation system consisting of a friction pendulum system (FPS) and a magnetorheological (MR) damper has been investigated. A fuzzy logic controller (FLC) is used to modulate the MR damper so as to minimize structural acceleration while maintaining acceptable base displacement levels. To this end, a multi-objective optimization scheme is used to optimize parameters of membership functions and find appropriate fuzzy rules. To demonstrate effectiveness of the proposed multi-objective genetic algorithm for FLC, a numerical study of a smart base isolation system is conducted using several historical earthquakes. It is shown that the proposed method can find optimal fuzzy rules and that the optimized FLC outperforms not only a passive control strategy but also a human-designed FLC and a conventional semi-active control algorithm.

***Keywords*—**Fuzzy logic controller, genetic algorithm, MR damper, smart base isolation system

I. Introduction

SMART base isolation strategy has been widely studied as a novel mitigation system to reduce structural damage caused by severe loads. Current literature shows that a smart base isolation system can reduce base drifts without accompanying increases in acceleration that are seen with passive strategies. In other words, active and semi-active strategies can provide reduced base drift without unacceptable superstructure motion. A number of studies have focused on the use of active control devices in parallel with a base isolation system for limiting base drift [1]-[5]. However, active control devices have yet to be fully embraced by practicing engineers in large part due to the challenges of large power requirements, concerns about stability and robustness, and so forth.

To overcome this problem, several researchers have investigated the use of semi-active smart dampers for seismic response mitigation as a component of a hybrid control system [6]-[9]. It has been shown that smart base isolation can protect a structure from extreme earthquakes without sacrificing performance during more frequent, moderate seismic events.

The structural designer usually has to ensure that both the safety of the structure, which mainly depends on the displacement response, and the comfort level of the occupants, which depends on the acceleration response, are within permissible limits. However, the first objective (reduction of displacement) is in conflict with the second one (reduction of acceleration). For example, if the resisting force of an MR damper in a smart base isolation system is increased in order to reduce base drift, the acceleration of the superstructure manifests a concomitant increase. In the opposite case, structural acceleration may be reduced by decreasing the structural stiffness, while the base drift may increase. This kind of problem can be solved using multi-objective optimization techniques that provide a suite of Pareto-optimal solutions. Schaffer [10] first proposed genetic algorithms as a multi-objective optimizer. However, the first Pareto-based multi-objective evolutionary algorithm to be published was the multi-objective genetic algorithm (MOGA) developed by Fonseca and Flemming [11]. Genetic algorithms are suitable search engines for multi-objective problems primarily because of their population-based approach. Because of the inherent robustness and ability to handle nonlinearities and uncertainties, FLC is used in this numerical study to operate a large MR damper, which is a key component of the smart base isolation system. More explicitly, a FLC design approach that uses MOGA for a smart base isolation system is employed to find a set of Pareto optimal solutions. Especially, a fast elitist non-dominated sorting genetic algorithm (NSGA-II) [12] is employed among various MOGAs in this study. Parameters from a large-scale experimental model are employed as the basis for numerical simulation. The large-scale experimental test was conducted at the National Center for Research on Earthquake Engineering (NCREE) in Taipei, Taiwan. The experimental model consists of a friction pendulum system (FPS) and a controllable magnetorheological (MR) damper. Powerful modelling capabilities of an adaptive neuro-fuzzy inference system (ANFIS) are used to develop a nonlinear neuro-fuzzy model of a large MR damper and four novel FPSs that support the mass. The neuro-fuzzy model represents dynamic behavior of a 300-kN MR damper for various displacement, velocity, and voltage combinations that are obtained from a series of performance tests. Modelling of the FPS is carried out with a nonlinear analytical equation and neuro-fuzzy training. Finally, a passive damping strategy, human-designed FLC, and a conventional semi-active controller (i.e. skyhook) are used to compare with the efficiency of several proposed optimal FLCs obtained using the NSGA-II algorithm. Based on computed responses to several historical earthquakes, the proposed approach is shown to provide efficiently a set of Pareto optimal FLCs for a smart base isolation system.

II. Multiple Objectives of Optimization

The fitness function provides an important connection between the GA and the physical system that is being modeled. As stated earlier an effective base isolation system simultaneously reduces base drift and structural acceleration thereby limiting or avoiding damage, not only to the structure but also to its contents.

H. S. Kim is with the Division of Architecture, Sunmoon University, Asan-si, 336-708 Korea (phone: 041-530-2315; fax: 041-530-2839; e-mail: hskim72@ sunmoon.ac.kr).

Therefore, the objectives in the design of a FLC for a smart base isolation system are to minimize both base drift and structural acceleration. In order to optimize a FLC for controlling a smart base isolation system, root mean squared (RMS) structural accelerations and base drifts that are normalized with respect to the uncontrolled RMS acceleration and drift responses, respectively, are used as the objective functions as well as normalized peak acceleration and drift responses. A summary of the objectives used in this study is given in Table 1, where, d is controlled base drift, $\hat{d}$ is uncontrolled base drift, a is controlled acceleration, $\hat{a}$ is uncontrolled acceleration, σ_d is controlled RMS base drift, $\sigma_{\hat{d}}$ is uncontrolled RMS base drift, σ_a is controlled RMS acceleration and $\sigma_{\hat{a}}$ is uncontrolled RMS acceleration. The maximum value is obtained from the structural response to a series of historical earthquakes and is selected as the value of the corresponding objective function. Here, 'uncontrolled' means a 'passive off' case for which the MR damper is installed in a smart base isolation system but no command voltage is sent to the damper. Later, a 'passive on' case is discussed for which the maximum command voltage is sent to the MR damper.

III. Smart Base Isolation System

A. Configuration of Smart Base-isolation System

A series of large-scale experimental tests on a smart base isolated system was conducted at NCREE. The smart base isolation system consists of a set of four specially-designed FPSs and an MR damper as shown in Fig. 1. Effectiveness of the hybrid base isolated system was experimentally verified. The system reduced base drifts without increasing accompanying accelerations during control using a human-designed FLC [13]. Although a knowledge-based FLC designed by an expert controls the smart base isolation system effectively in comparison with passive control strategies during experimental tests, there seems to be considerable room for improvement through use of an optimal design method. Therefore, this experimental model of a smart base isolation system is employed as a numerical example in order to demonstrate improved performance of the FLC by using the proposed design approach.

TABLE I
Objectives of FLC optimization for smart base isolation system

Description	Objectives
Normalized Peak Base Drift	$f_{peak\_drift} = \max_{earthquakes}\left\{\frac{\max_t\lvert d(t)\rvert}{\max_t\lvert\hat{d}(t)\rvert}\right\}$
Normalized Peak Acceleration	$f_{peak\_accel} = \max_{earthquakes}\left\{\frac{\max_t\lvert a(t)\rvert}{\max_t\lvert\hat{a}(t)\rvert}\right\}$
Normalized RMS Base Drift	$f_{RMS\_drift} = \max_{earthquakes}\left\{\frac{\sigma_d(t)}{\sigma_{\hat{d}}(t)}\right\}$
Normalized RMS Acceleration	$f_{RMS\_accel} = \max_{earthquakes}\left\{\frac{\sigma_a(t)}{\sigma_{\hat{a}}(t)}\right\}$

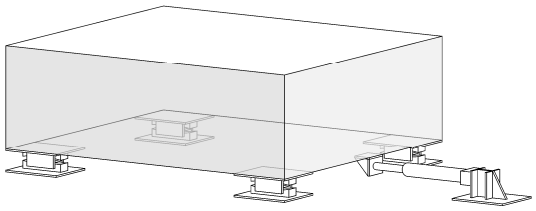

Fig. 1 Configuration of smart base-isolation system

The isolated structure is constructed with a steel frame and lead blocks that provide a 24,000-kg mass that behaves as a single degree of freedom. A 300-kN MR damper that is used numerical simulation of control in the following sections (see Fig. 2(a)), was manufactured by Sanwa Tekki Corporation, Tokyo, Japan. Four identical FPSs support the mass as shown in Fig. 2(b). Advantages of a base isolation system that employs FPSs include generation of recentering forces, simple numerical modeling, and an isolated structure that has a constant period regardless of the mass that the FPS supports. Furthermore, the center of lateral rigidity of the isolation system coincides with the center of mass of the structure. This property makes the FPS bearings particularly effective at minimizing adverse torsional motion in asymmetric structures.

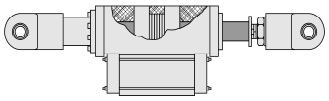

(a) 300-kN MR damper

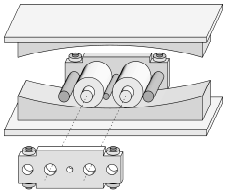

(b) FPS with dual rollers

Fig. 2 Hardware devices used in hybrid base-isolated system

B. Modeling of MR Damper

Extensive performance testing of a 300-kN MR damper was conducted at NCREE using a dynamic actuator to collect a sufficient quantity of data that are evenly distributed over the operational range of the MR damper. These data enable training of neuro-fuzzy model that can be used to numerically simulate dynamic behavior of the damper. Special properties of an MR damper include relationships of parameters such as displacement, velocity, applied voltage, and resisting force.

Because this model has been shown to provide sufficient information for operation of the damper and is suitable for control purposes [14], these three input and force output parameters are used in what follows to model the 300-kN MR damper.

Experimental data for MR damper modeling are divided into the following two parts: (1) training and checking, and (2) validation. Training data are used to learn and adjust the fuzzy rules while checking data verify that the model is not overfitted.

Later, validating data are applied to the trained fuzzy model to substantiate whether or not the model is suitable when unknown input data are applied and the force in the MR damper is to be predicted. All data sets from performance tests are concatenated in preparation for training and validation of a neuro-fuzzy model. After training and checking data for the MR damper are defined, they are presented to a neuro-fuzzy algorithm in order to train a target model. All numerical simulations for training a damper model are made by using the fuzzy logic toolbox of MATLAB. After extensive training through ANFIS, a satisfactory fuzzy model of the MR damper is obtained as shown in Fig. 3 [14]. The fuzzy inference system (FIS) that represents behavior of the 300-kN damper has 2, 4, and 3 membership functions for the displacement, velocity, and voltage, respectively, and has a total of 24 rules.

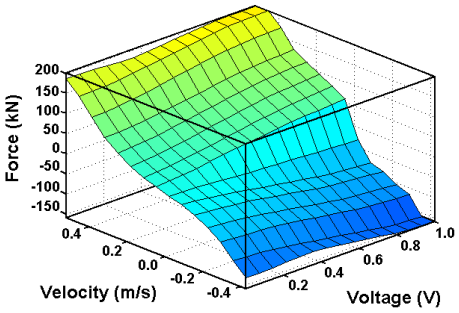

Fig. 3 Fuzzy inference surface of trained MR damper model

C. Modeling of FPS

An FPS is a mechanical device that isolates a structure from its support. Four FPSs are used to support the mass of the structure as shown in Fig. 1; that is, they serve as an interface between the structure and the ground. During an earthquake FPSs are used to achieve any desired range of motion. This can be accomplished by altering the bearing material or by changing the radius of curvature of the spherical surface. For all data generated in this paper the coefficient of friction is taken to be 0.03 and the radius is set at 1.0 m. In order to establish pseudo-experimental data (i.e. data that can be taken as sufficiently similar to experimental behavior) that describes the nonlinear force-displacement relationship of a typical FPS system, the following equation can be employed. This equation is established by a simple analytical relationship from fundamental principles of mechanics [15].

$$F = W\left[\frac{u + \mathrm{sgn}(\dot{u})\mu\sqrt{R^2 - u^2}}{\sqrt{R^2 - u^2} - \mathrm{sgn}(\dot{u})\mu u}\right] \quad (1)$$

where F is the external force acting on the FPS, R is the radius of the spherical bearing surface, u is horizontal displacement, $\dot{u}$ is horizontal velocity, μ is the coefficient of friction, sgn indicates a positive or negative sign of its function, and W is the weight of the mass supported by the FPS. Here, ANFIS is also used to develop a neuro-fuzzy model of the FPS. The FIS for the FPS is designed with two inputs (displacement and velocity) and a single output (damping force) based on (1). A sufficiently long history of white noise minimizes the amount of interpolation required by a fuzzy model of the FPS, thus increasing accuracy of force prediction within the actual range of operation. Fuzzy inference surfaces that represent evaluation of the membership functions for a range of input variables are shown in Fig. 4.

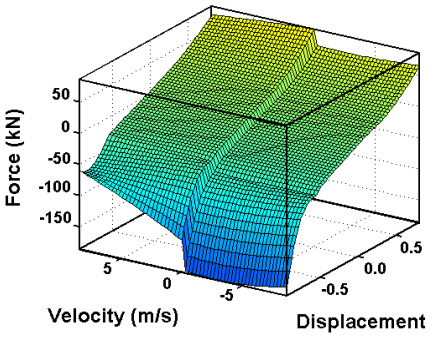

Fig. 4 Fuzzy inference surface for FPS model with μ = 0.03.

IV. Comparative Controllers

A. Human-designed FLC

In order to verify control performance of the NSGA-II-optimized FLC, a comparative FLC is used that is based on the knowledge of a human expert. The absolute acceleration and base drift of the structure are selected as inputs and the output is the command voltage. The fundamental approach to design of the human-designed FLC is to minimize both the structural acceleration and the base drift of the isolated structure. As a result, this controller divides the response of the isolation system into three types. First, when the absolute acceleration is very large, the command voltage is specified to be small when base drift is small and large when the base drift is very large. In this situation, the command voltage is suppressed to prevent excitation of the acceleration responses except when the base drift is also very large. Secondly, when the absolute acceleration is small, the command voltage is increased in proportion to the base drift. That is, the command voltage is as large as possible except for the small response zone. Thirdly, when the absolute acceleration is almost zero, the command voltage is zero when base drift is small and small when the base drift is large. This approach provides a zero command voltage zone around acceleration responses that are minuscule and softens the MR damper when seismic excitation is very small. Fig. 5 shows the corresponding control surface.

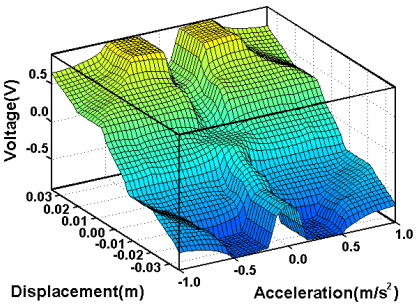

Fig. 5 FIS surface for human-designed FLC

B. Skyhook Controller

A skyhook controller is also employed for comparison with the human-designed FLC and the NSGA-II controller. As opposed to conventional dampers that tend to reduce the relative acceleration of the mass, the skyhook controlled damper attempts to reduce absolute acceleration of the mass [16]. As the damping coefficient of the skyhook damper is optimized, the response of the system near its resonant frequency is reduced and the response at higher frequencies also can be reduced somewhat. By contrast, in a conventional damper, a reduced response at resonant frequency is obtained at the cost of degraded response at higher frequencies. The skyhook control algorithm used in this study is given by the following:

$$V(t) = \begin{cases} V_{\max} & \text{if } \dot{u}_a \dot{u}_r > 0 \\ V_{\min} & \text{if } \dot{u}_a \dot{u}_r < 0 \end{cases} \quad (2)$$

where, $V(t)$ is the command voltage; $V_{\max}$ is the maximum voltage, namely 1 V; $V_{\min}$ is the minimum voltage, 0 V; $\dot{u}_a$ is the absolute velocity and $\dot{u}_r$ is the relative velocity.

V. Numerical Results

A numerical model of the smart base isolation system with a FPS and MR damper is implemented in SIMULINK as shown in Fig. 6. Quantization error and saturation of the analog to digital converter (ADC) and digital to analog converter (DAC) and sensor noise have been included in the SIMULINK model in order to simulate a realistic representation of the control system. The ADC and DAC have 16-bit precision, a span of ±10 V, and sensor noise of 0.03 V RMS, i.e. 0.3% of the range of the ADC signal. Excitation records that are used for numerical simulation include three commonly used earthquakes: El Centro (18 May 1940), Kobe (17 January 1995) and Northridge (17 January 1994). An integration time step of 0.01 sec is used and the control signal is computed every 0.01 sec. An implementation of NSGA-II is employed for optimization of the control system. A flowchart of the NSGA-II based optimization is presented in Fig. 7. Several optimization parameters need to be determined before starting the optimization run. Here, the population size is taken to contain 100 individuals. An upper limit on the number of generations is specified to be 500. When the optimization is started, NSGA-II generates an initial population of chromosomes, each of which represents a FLC. Numerical simulation of the smart base isolation system is conducted a total of 100 times using the concatenated earthquake records and the control performance of each FLC is evaluated. Next, NSGA-II creates a new generation of chromosomes based on multi-objective ranking using a several simple GA operators such as selection, crossover, and mutation. First, only two peak objectives (i.e., f_{peak_drift} and f_{peak_accel}) out of four objectives introduced in Table I are used for multi-objective optimization of FLC and a Pareto optimal front (a set of Pareto optimal solutions) is found as shown in Fig. 8. Control performances of comparative controllers are also investigated. Optimization results from the human-designed FLC, a passive-on controller, and the skyhook controller are shown in Figs. 8 through 10. The passive-on case can be thought of as the best passive case for the reduction of base drift because the capacity of the MR damper is fully employed. As expected, normalized peak and RMS base drift for the passive-on case are smaller than those of the human-designed FLC and the skyhook controller. On the other hand, the skyhook controller shows better performance in reducing normalized structural acceleration in comparison with the passive-on case due to its fundamental design concept. It can be seen that the control performance of the human-designed FLC is intermediate between passive-on and skyhook controller results; namely, it can reduce base drift better than the skyhook controller and it reduces structural acceleration better than the passive-on controller.

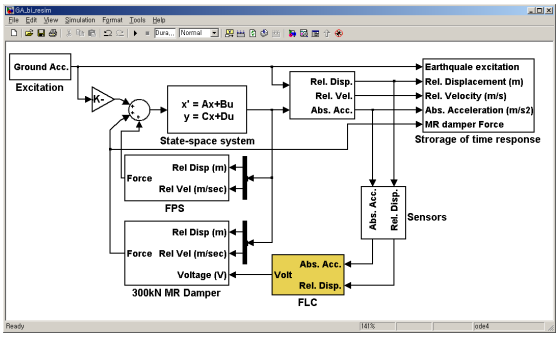

Fig. 6 SIMULINK block diagram for the smart base isolation system

Performances of the NSGA-II-optimized FLCs are found to be far better in controlling peak responses of the isolated structure than those of comparative controllers as shown in Fig. 8(a). Non-dominated individuals in the population of the 500th generation are presented in graphs as blank circles. However, NSGA-II-optimized FLCs do not provide very good control performances for RMS responses as shown in Fig. 8(b) because only two peak objectives are employed in the optimization process as mentioned previously. There is no individual that can appropriately reduce both normalized RMS base drift and normalized RMS structural acceleration. It can be seen that non-dominated individuals are separated into two groups. Here, one group effectively controls RMS base drift but sacrifices control of RMS acceleration while the other group effectively reduces RMS acceleration while sacrificing RMS base drift.

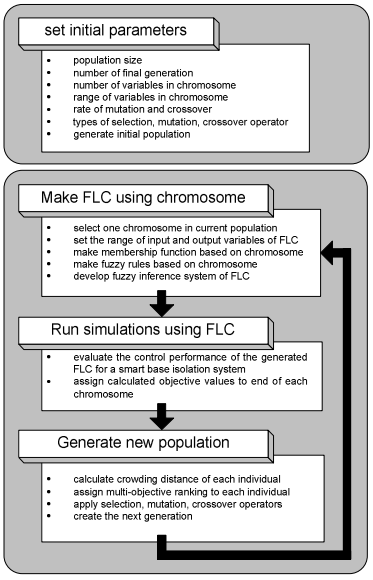

Fig. 7 Flowchart of NSGA-II based optimization

Next, optimization results with two RMS objectives are presented in Fig. 9. In the case of RMS responses, NSGA-II provides a set of Pareto optimal FLCs that have better control performances in comparison with other controllers as presented in Fig. 9(b). Also, it can be seen that control performances of optimal FLCs are superior to those of NSGA-II FLCs shown in Fig. 8(b). Fig. 9(a) shows peak responses of FLCs optimized by RMS objectives. Control performances of these RMS-optimized FLCs are inferior to those obtained from the FLCs optimized by peak objectives shown in Fig 8(a). However, these RMS-optimized FLCs can reduce peak responses more effectively than comparative controllers and yet they retain outstanding control performances for RMS responses.

Finally, control performances of a set of FLCs that are optimized by all four objectives introduced in Table 1 are presented in Figure 10. FLCs optimized by all four objectives effectively reduce peak and RMS responses simultaneously in comparison with the other controllers although control performance of peak or RMS responses of these FLCs is inferior to that obtained from the FLCs that are optimized using only two peak or two RMS objectives, respectively. In general, displacement responses are in competition with acceleration responses. Thus, the objectives f_{peak_drift} and f_{RMS_drift} can be improved at the cost of the degraded objectives f_{peak_accel} and f_{RMS_accel}, respectively. Therefore, an engineer needs to choose a proper FLC that can satisfy the desired performance requirements.

While the number of non-dominated individuals obtained after optimization with two peak or RMS objectives is 41 and 43, respectively, the number of non-dominated individuals optimized by all four objectives is 73. That is, the percentage of elite solutions is large compared to the population size (100). In the case of multi-objective optimization, the meaning of elite solutions is different from that in single objective optimization. Here all solutions that belong to the currently-best non-dominated front are best solutions in the population and are all equally important. Thus, all these solutions are elite solutions. In some cases, a population may be mostly comprised of currently-best non-dominated solutions. The percentage of non-dominated solutions increases as the number of multi-objectives increases. When this happens, the preservation of elitism means acceptance of all such solutions. In such a scenario, not many new solutions can be accepted in the population. As a result, the search process may stagnate or prematurely converge to a suboptimal solution set. Thus, there may be a need to increase the population size or introduce elitism in a controlled manner in the multi-objective optimization.

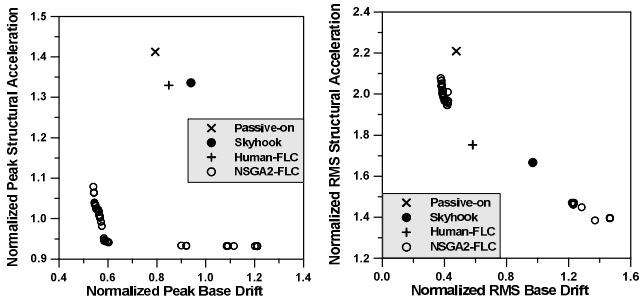

(a) peak responses (b) RMS responses

Fig. 8 Optimization results with two peak objectives

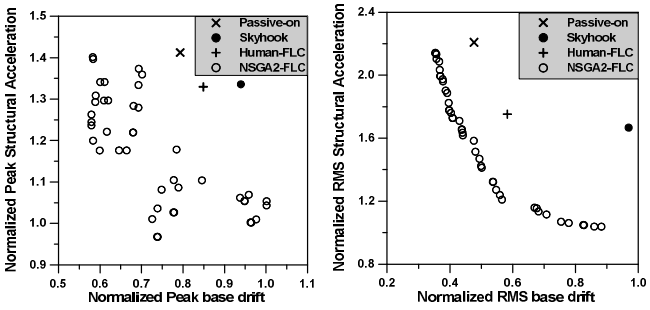

(a) peak responses (b) RMS responses

Fig. 9 Optimization results with two RMS objectives

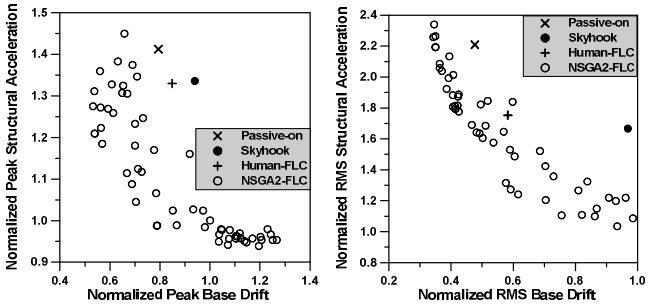

(a) peak responses (b) RMS responses

Fig. 10 Optimization results with four objectives

In summary, to minimize peak structural responses regardless of RMS responses, a design engineer can choose the most appropriate FLC from among the set of FLCs presented in Fig. 8(a) that corresponds with a given design objective. However, if an engineer wants to appropriately control RMS

responses with some sacrifice in the control of peak responses, the most appropriate FLC can be selected from among non-dominated solutions shown in Fig. 10.

VI. Conclusion

This study investigates the performance of an MOGA-optimized FLC for a smart base isolation system consisting of an FPS isolator and a large MR damper. A fast elitist non-dominated sorting genetic algorithm (NSGA-II) is employed to find a set of Pareto optimal solutions representing FLCs. Reduction of base drifts and structural acceleration of the smart base isolation system are selected as multiple objectives. After an optimization run using NSGA-II, the engineer can choose an appropriate FLC that satisfies the desired performance requirements from among a number of optimal solutions. By comparison, in order to determine a set of optimal solutions using the classical method of combining multiple objectives such as the weighted sum approach, a number of optimization runs are necessary because only a single optimal solution can be obtained through one optimization run. However, NSGA-II can provide multiple Pareto optimal solutions in one single run.

Passive, skyhook, and a human-designed FLC are used as comparative controllers to investigate the effectiveness of the NSGA-II-optimized FLC. In the passive-on control case, base drift can be significantly reduced but structural acceleration is not well controlled. The skyhook controller reduces structural acceleration in comparison with passive-on control, but only at the expense of larger base drifts for all earthquakes that are numerically simulated. A human-designed FLC can reduce base drift better than the skyhook approach and it can reduce structural acceleration better than passive-on operation of the MR damper. That is, a human-designed FLC can appropriately control both base drift and structural acceleration. Finally, a NSGA-II-optimized FLC shows better performance in comparison with all of the comparative controllers.

Normalized RMS responses as well as normalized peak responses are used as objective functions in multi-objective optimization in this study. When only RMS or peak responses are employed in the optimization process, corresponding responses can be outstandingly controlled relative to the control that is obtained with all of the comparative controllers, whereas other response metrics that are excluded from the optimization process are not controlled very well. When all of the RMS and peak responses are employed in the optimization process, a set of optimal FLCs that can effectively reduce both RMS and peak responses simultaneously in comparison with the other controllers can be found. Based on these numerical studies, a smart base isolation system consisting of an MR damper and a novel FPS with an appropriate controller is shown to be capable of achieving significant decreases in base drift without accompanying increases in acceleration that occur in passive base isolation systems.

Acknowledgment

This work was supported by the National Research Foundation of Korea (NRF) grant funded by the Korea government (2011-0015166).

References

[1] J. M. Kelly, G. Leitmann, and A. G. Soldatos, "Robust control of base-isolated structures under earthquake excitation," *Journal Optimization Theory and Applications*, vol. 53, 1987, pp. 159-180.

[2] S. Nagarajaiah, M. A. Riley, and A. Reinhorn, "Control of sliding-isolated bridge with absolute acceleration feedback," *Journal of Engineering Mechanics*, vol. 119, 1993, pp. 2317-2332.

[3] W. E. Schmitendorf, F. Jabbari, and J. N. Yang, "Robust control techniques for buildings under earthquake excitation," *Earthquake Engineering and Structural Dynamics*, vol. 23, 1994, pp. 539-552.

[4] J. N. Yang, J. C. Wu, A. M. Reinhorn, and M. Riley, "Control of sliding-isolated buildings using sliding-mode control," *Journal of Structural Engineering*, vol. 122, 1996, pp. 179-186.

[5] K. Yoshida, S. Kang, and T. Kim, "LQG control and H` control of vibration isolation for multi-degree-of-freedom systems," *Proceedings of the First World Conference on Structural Control*, Los Angeles, CA, TP4, 1994, pp. 43-52.

[6] E. A. Johnson, and J. C. Ramallo, B. F. Spencer, Jr., and M. K. Sain, "Intelligent base isolation systems," *Proceedings of the 2nd World Conference on Structural Control*, Kyoto, Japan, 1999, pp. 367-376.

[7] N. Kurata, T. Kobori, M. Takahashi, N. Niwa, and M. Hiroshi, "Actual seismic response controlled building with semi-active damper," *Earthquake Engineering and Structural Dynamics*, vol. 28, 1999, pp. 1427-1447.

[8] M. D. Symans, and M. C. Constantinou, "Semi-active control systems for seismic protection of structures: A state-of-the-art review," *Engineering Structures*, vol. 21, 1999, pp. 469-487.

[9] N. Niwa, T. Kobori, M. Takahashi, Y. Matsunaga, N. Kurata, and T. Mizuno, "Application of semi-active damper system to an actual building," *Proceedings of the Second World Conference on Structural Control*, Kyoto, Japan, 1999, pp. 815-824.

[10] J. D. Schaffer, "Multiple objective optimization with vector evaluated genetic algorithms," *Proceedings of the First International Conference on Genetic Algorithms*, Hillsdale, NJ, 1985, pp. 93-100.

[11] C. M. Fonseca, and P. J. Fleming, "Genetic algorithms for multiobjective optimization: Formulation, discussion and generalization," *Genetic Algorithms: Proceedings of the Fifth International Conference*, Morgan Kaufmann, San Mateo, CA, 1993, 416~423.

[12] K. Deb, A. Pratap, S. Agrawal, and T. Meyarivan, "A fast elitist non-dominated sorting genetic algorithm for multi-objective optimization: NSGA-II," Technical Report No. 200001, Kanpur: Indian Institute of Technology Kanpur, India, 2000.

[13] P. Y. Lin, P. N. Roschke, C. H. Loh, and C. P. Cheng, "Semi-active controlled base-isolation system with magnetorheological damper and pendulum system," *Proceedings of the 13th World Conference on Earthquake Engineering*, Vancouver, British Columbia, Canada, 2004.

[14] V. Likhitruangsilp, "Neuro-fuzzy control based of a multi-degree of freedom structure with semi-active magnetorheological dampers," MS Thesis, Department of Civil Engineering, Texas A&M University, College Station, TX. 2002.

[15] H. S. Kim, P. N. Roschke, P. Y. Lin, and C. H. Loh, "Fuzzy control of a novel base isolator and MR damper for seismic applications," *Engineering Structures*, vol. 28, 2006, pp. 947-958.

[16] D. Karnopp, M. J. Crosby, and R. A. Harwood, "Vibration control using semi-active force generators," *Journal of Engineering for Industry, ASME*, vol. 96, 1974, pp. 619-626.